Dalton Transactions

Cite this: DOI: 10.1039/c2dt31570j

www.rsc.org/dalton

PAPER

Synthesis, characterization and antitumor activity of new ferrocene incorporated *N*,*N*′-disubstituted thioureas†

Bhajan Lal,[a,b] Amin Badshah,*[a] Ataf Ali Altaf,[a,c] Muhammad Nawaz Tahir,[d] Shafiq Ullah[a] and Fazlul Huq*[b]

Received 16th July 2012, Accepted 19th September 2012
DOI: 10.1039/c2dt31570j

We report herein the synthesis, structural characterization and activity against human ovarian tumour models: A2780 (parent), A2780^{cisR} (resistant to cisplatin) and A2780^{ZD0473R} (resistant to the cisplatin analogue denoted as ZD0473) of two ferrocene incorporated *N*,*N*′-disubstituted thioureas {1-benzoyl-3-(4-ferrocenylphenyl)thiourea, B16, and 1-acetyl-3-(4-ferrocenylphenyl)thiourea, B3}. Structural characterization has been based on FT-IR, multinuclear (^{1}H and ^{13}C) NMR, elemental analysis and single crystal X-ray diffractometry. Ferrocene-incorporated thioureas may present themselves as a new class of metal-based tumour active compounds. The cyclic voltammetric measurements indicate that B16 undergoes partial intercalation with the CT-DNA whereas B3 undergoes only electrostatic interaction with the same. Partial prevention of BamH1 digestion of pBR322 plasmid DNA that has been interacted with high concentrations of both B16 and B3 indicates that even non-covalent interactions can induce significant conformational changes in the DNA.

Introduction

Although platinum drugs cisplatin, carboplatin and oxaplatin are routinely used in the clinic to kill cancerous cells, their use has also been limited due to inherent and acquired resistance and the presence of a number of dose-limiting side effects.[1,2] The cytotoxic effect of the compounds is related to their interaction with the DNA that ultimately inhibits the transcription and replication resulting in cell death.[3–9] The search for better metal-based drugs having the ability to overcome problems of drug resistance and side effects associated with platinum based chemotherapy constitutes the foundation of bio-organometallic chemistry. Ferrocene and its derivatives have been excessively studied as potential chemotherapeutics.[10–12] The stability, electroactivity and high spectroscopic activity of ferrocene based organometallics make them promising candidates for many biological applications.[13] The presence of the ferrocenyl moiety enhances activity due to its reversible redox behaviour and increases cell permeability due to its lipophilic nature.[14] It has been reported that when ferrocene was incorporated into tamoxifen, the anticancer activity of the drug is enhanced.[15] Ferrocene derivatives may bind with the DNA *via* both covalent and noncovalent modes of interaction. The anticancer activity of ferrocene derivatives is found to be dependent on the oxidation state of iron in the ferrocene moiety with some results indicating that the Fe(II) ferrocenyl compound is more active than Fe(III) ones.[16] The results of the study on ferrocifen as one of the Fe(II) compounds indicate that the ferrocifens act by changing the conformation of the receptor protein.[17] Binding of ferrocifen to ERβ is thought to lead to its dimerization followed by attachment of the dimerized species to a particular region of DNA. The electron transfer reaction involving the ferrocenium ion *in vivo* or the ferrocifen–ERβ complex may generate reactive oxygen species (ROS) such as hydroxyl radicals (˙OH). ROS produced can cause damage to DNA[18] and may also be responsible for anticancer activity through the formation of radical metabolites that bring about biological damage in the cancer cell.[19]

Thiourea-based complexes have also been screened for various biological activities.[20] The presence of the thiocarbonyl moiety influences the lipophilicity/hydrophilicity and the electronic properties of the compounds affect the lability of the leaving groups thus controlling the biochemical action.[13] Several thiourea derivatives have shown potential antitumour activity because of their inhibitory response against receptor tyrosine kinases (RTKs), protein tyrosine kinases (PTKs) and NADH oxidase.[21,22] Herein we report the synthesis, structural characterization, anticancer activity and extent of DNA binding of two ferrocene incorporated *N*,*N*′-disubstituted thioureas.

Results and discussion

Synthesis and characterization

Two ferrocene incorporated *N*,*N*′-disubstituted thioureas coded as B16 and B3 have been synthesized by allowing 4-ferrocenyl

[a]*Department of Chemistry, Quaid-i-Azam University, Islamabad-45320, Pakistan. E-mail: aminbadshah@yahoo.com; Fax: +92 51 9064 2241; Tel: +92 51 9064 2131*
[b]*Discipline of Biomedical Sciences, The University of Sydney, Sydney, Australia. E-mail: Fazlul.Huq@sydney.edu.au; Fax: +61 2935 19520; Tel: +61 2935 19522*
[c]*Department of Chemistry, University of Malakand, Chakdara, Dir (lower), Pakistan*
[d]*Department of Physics, University of Sargodha, Sargodha, Pakistan*
†CCDC 889603–889604. For crystallographic data in CIF or other electronic format see DOI: 10.1039/c2dt31570j

aniline to react with freshly prepared acetyl and benzoyl isothiocyanates under a N_2 atmosphere in dry acetone (Scheme 1). The compounds have been characterized based on FT-IR, ^{1}H and ^{13}C NMR, elemental analysis and single crystal XRD.

FT-IR spectra showed a broad peak for the N–H stretch in the range of 3300–3430 cm^{-1} due to involvement of hydrogen bonding and secondary bonding interactions that are confirmed by the crystal structures. The peak in the range of 1650–1700 cm^{-1} is assigned to (C═O) while that at 1130–1270 cm^{-1} is assigned to (C═S). The aliphatic and aromatic protons appeared at the normal range of 2850–3050 cm^{-1}. In ^{1}H NMR spectra ferrocenyl protons appear at 4–5 ppm. In the ^{13}C NMR spectra the (C═O) and (C═S) peaks appear at 160–185 ppm whereas ferrocenyl carbons appear at 60–90 ppm. The aromatic and aliphatic protons and carbons appear in the usual regions in ^{1}H and ^{13}C NMR.[12,23]

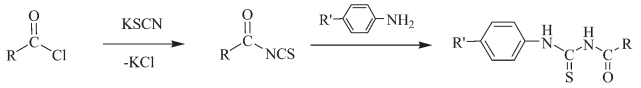

Compounds	R	R'
B16	Phenyl	Ferrocenyl
B3	Methyl	Ferrocenyl

Scheme 1 Synthesis of ferrocenyl thioureas.

Table 1 Crystal data and structure refinement parameters for B16 and B3

Crystal parameters	B16	B3
Empirical formula	$C_{24}H_{20}FeN_2OS$	$C_{19}H_{18}FeN_2OS$
Formula weight	440.34	378.27
Temperature (K)	296	296
Wavelength (Å)	0.71073	0.71073
Crystal system	Monoclinic	Triclinic
Space group	*P*21/*c*	*P*$\bar{1}$
Unit cell dimensions		
a (Å)	11.0296(4)	8.0003(4)
b (Å)	31.5720(13)	11.0413(6)
c (Å)	12.3030(5)	19.8358(12)
α (°)	90	81.868(4)
β (°)	103.412(2)	80.899(3)
γ (°)	90	86.194(4)
V (Å^3), *Z*	4167.4(3), 8	1710.98, 4
Density (g cm^{-3})	1.404	1.469
Crystal size (mm^3)	40 × 210 × 15	39 × 24 × 18
Index ranges	$(h,k,l)_{max}$ (14,42,16) $(h,k,l)_{min}$ (−14, −42, −16)	$(h,k,l)_{max}$ (9,13,23) $(h,k,l)_{min}$ (−9, −13, −23)
Total reflections	10 405	6192
μ (mm^{-1})	0.841	1.011
R indices (all data)	0.1672	0.1578
Final *R* indices [$I > 2\sigma(I)$]	0.0580	0.0585
Goodness-of-fit	0.966	0.969
θ range (°)	1.29–28.33	2.10–25.25

Single crystal X-ray studies

Careful crystallization of B16 and B3 in ethyl acetate by slow evaporation yielded orange crystals suitable for single crystal X-ray diffraction analysis. Data pertaining to the data collection and structure refinement are given in Table 1.

Table 2 provides a selection of some important interatomic distances, bond angles and torsion angles. Fig. 1 and 2 represent the molecular structures with the numbering scheme of B16 and B3 respectively. The intra-molecular hydrogen bonding and intermolecular interactions present in these compounds are summarized in Table 2 and drawn in Fig. 3 and 4.

In B16, the rings A (C6–C10), B (C11–C16), C (H1A, N1, C17, N2, C18 and O) and D (C19–C24) are planar with r.m.s. deviations of 0.0016, 0.0043, 0.0416 and 0.0084 respectively. All these four planes are on the same surface due to the extended

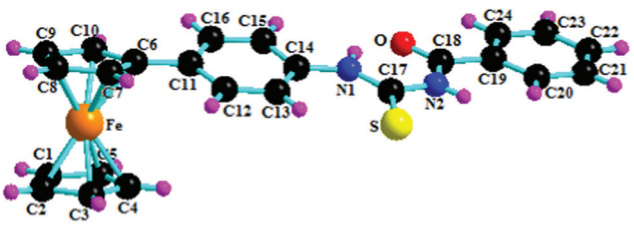

Fig. 1 Molecular structure of B16.

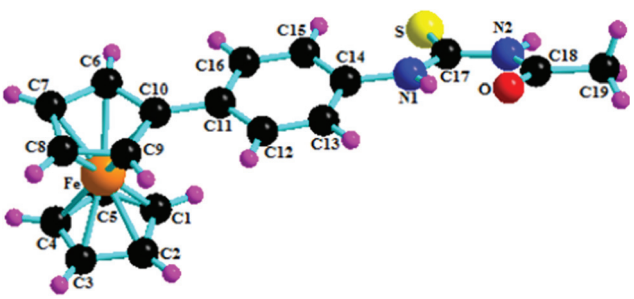

Fig. 2 Molecular structure of B3.

Table 2 The intra-molecular and intermolecular hydrogen bond interactions in B16 and B3

Compound	X	H	Y	*d*(X–H) (Å)	*d*(H–Y) (Å)	*d*(X–Y) (Å)	∠(XHY) (°)
Intra-molecular hydrogen bonds							
B16	O1	H1A	N1	1.864(3)	0.861(3)	2.602(5)	142.69(23)
B3	O1	H1A	N1	1.925(4)	0.859(5)	2.648(6)	140.99(29)
Intermolecular hydrogen bonds							
B16	S	H20	C20	2.993	0.929(4)	3.269	98.95
	S	H2A	N2	2.571	0.860(3)	3.376	156.46

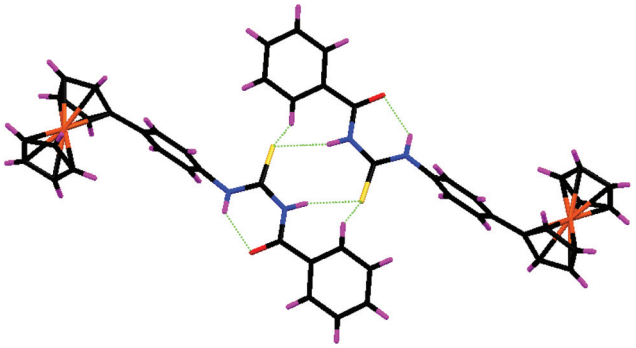

Fig. 3 Inter- and intra-molecular hydrogen bonding in B16.

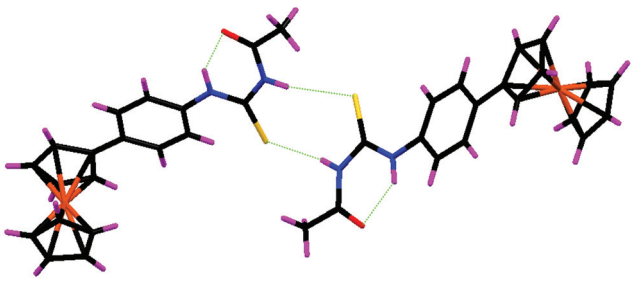

Fig. 4 Inter- and intra-molecular hydrogen bonding in B3.

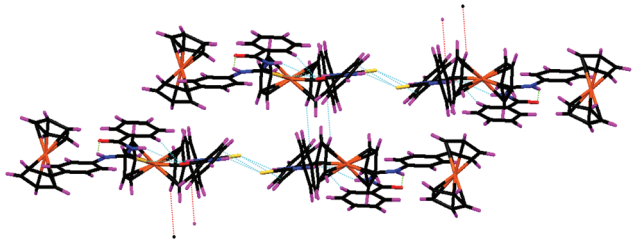

Fig. 5 Supramolecular structures of B16 mediated by secondary bonding.

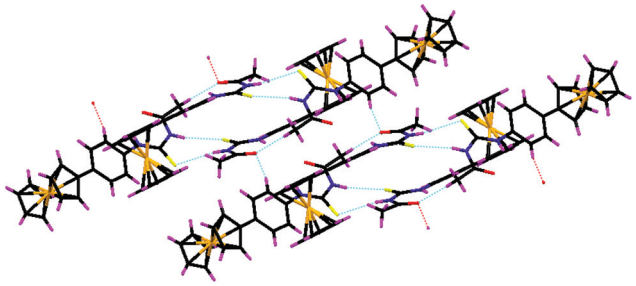

Fig. 6 Supramolecular structures of B3 mediated by secondary bonding.

resonance over the twenty-three atoms in the molecule. The existence of intermolecular hydrogen bonding (NH···O type) is responsible for the planarity of six atoms forming ring C in B16 (Fig. 3). The interplanar angles between these planes are found to be A/B = 19.04, A/C = 15.80, A/D = 12.93, B/C = 7.55, B/D = 6.47, C/D = 4.71. In B3, the rings A (C6–C10), B (C11–C16) and C (H1A, N1, C17, N2, C18 and O) are planar with r.m.s. deviations of 0.0057, 0.0080 and 0.0174 respectively. In the case of B3, three planes are on the same surface due to the extended resonance over the sixteen atoms in the molecule. The interplanar angles between these planes are found to be A/B 3.87, B/C 21.70, C/A 25.46. The existence of intra-molecular hydrogen bonding (NH···O type) is responsible for the planarity of six atoms forming ring C in B3 (Fig. 4). This type of intra-molecular hydrogen bonding is well known for such kinds of aroyl or acoyl substituted organic thioureas as we found in the ferrocene analogues.[24–26]

The dihedral angle between rings A and B is larger in B16 than in B3, indicating the extended resonance among these rings in B3 which makes them more planar. It may be due to the attachment of the benzoyl group to the thiourea nitrogen which extends resonance in a direction opposite to the ferrocene. The acetyl group does not attract the electron charge density and allows the ferrocene to gain resonance electrons charge density and make the system more planar. The bond distances between A and B rings (C6–C11 = 1.477(6) in B16 and C10–C11 = 1.456(8) in B3) also anticipate the same stronger bond in B3. The two independent molecules exist in an asymmetric unit in both structures (B16 and B3) which are connected alternately to each other by the intermolecular hydrogen bonding of type NH···O, NH···S and secondary non-covalent interactions (π···H), to mediate a supramolecular structure for B16 and B3 as shown in Fig. 5 and 6. These kinds of secondary intermolecular non-bonding interactions are considered to be an important determinant of biological activities; compounds pertaining to stronger nonbonding interactions are found to have a greater ability to bind with macrobiological molecules such as proteins and DNA.[27] Among the compounds under study B16 is found to have more secondary interactions that are evident from hydrogen bonding data and supramolecular structure formation. Hence it is expected that B16 will associate with DNA more strongly that will translate into higher biological activities.

Cytotoxicity

The cytotoxicity of B16 and B3 along with that for cisplatin was screened against human ovarian cell lines: A2780 (parent), $A2780^{cisR}$ (cisplatin-resistant type), $A2780^{ZD0473R}$ (ZD0473-resistant type) by using the 3-(4,5-dimethylthiazol-2-yl)-2,5-diphenyltetrazolium bromide (MTT) reduction assay. The IC_{50} values meaning the concentrations of compounds (B16, B3 and cisplatin) required for 50% cell kill were determined and are listed in Table 4. B16 is found to be more active than B3 although B16 and B3 are less active than cisplatin against all the cell lines. However, B16 and B3 have lower resistance factors (Rf) than cisplatin such that the compounds are equally or nearly equally active against both the parent (A2780) and the resistant ($A2780^{cisR}$ and $A2780^{ZD0473R}$) cell lines. In contrast, cisplatin has much lower activity against the resistant cell lines than the parent cell line. The results indicate that at the level of their activity, B16 and B3 have been better able to overcome mechanisms of resistance operating in the cell lines. One possible reason for the difference in activity of B3 and B16 as compared to that for cisplatin may lie in the difference in the nature of interaction with the DNA.[28] Whereas cisplatin binds covalently with

nucleobases in the DNA, B16 is believed to undergo partial intercalation in between nucleobases in the DNA and B3 undergoes only electrostatic interaction with the same. In both B16 and B3, the antitumour effect is related to the oxidation state of the central iron atom of the ferrocenyl group. The low oxidation potential of B16 and B3 as compared to ferrocene supports the idea that the ferrocenyl moiety may be easily oxidized to the Fe^{3+} state. It is believed that it is mainly the Fe^{3+}-ferrocenyl cation that undergoes electrostatic interaction with the phosphate backbone of the DNA. As noted earlier, the electron transfer reaction involving Fe^{2+}- and Fe^{3+}-ferrocenyl species may generate ROS *in vivo* that cause damage to DNA.[19,29]

DNA binding studies

Voltammetric studies

The cyclic voltammetric measurements of 1 mM of B16 and B3 were performed in the absence and presence of calf thymus DNA (CT-DNA). On addition of increasing concentrations of CT-DNA (1 mL of 20 μM, 40 μM and 60 μM) into 1 mM B16 and B3 (Fig. 7 and 8), the shift in anodic potential and drop in i_{pa} are observed. The drop in current is attributed to diffusion of the drug into double helical DNA resulting in the formation of a supramolecular complex. The shift in formal potential reveals the mode of interaction between the drug and DNA.[30] Intercalation of the drug into the double helical structure of DNA causes a positive shift in the formal potential whereas a negative shift in the formal potential is indicative of the presence of electrostatic interaction of the cationic drug with the anionic phosphate of the DNA backbone. Thus the positive shift in formal potential observed for B16 after the addition of CT-DNA can be seen to indicate the occurrence of the intercalative mode of interaction.[31] However the ferrocene moiety cannot intercalate into the double helix because of its size but the remaining part of the molecule (most likely phenyl rings) can intercalate. B3 shows a negative shift in formal potential which is attributed to electrostatic interactions between the drug and the DNA. The shift in formal potential can be used to find out which form, ferrocene or

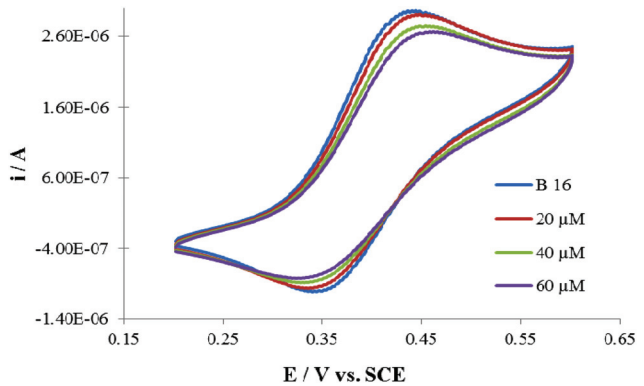

Fig. 7 Cyclic voltammograms of 1 mM B16 recorded at a 0.05 V s^{-1} potential sweep rate on a glassy carbon electrode at 298 K in the absence and presence of 1 mL of increasing concentrations of CT-DNA (10 μM, 20 μM and 60 μM) in a 20% aqueous DMSO buffer at pH 6.0; supporting electrolyte 0.1 M TBAP.

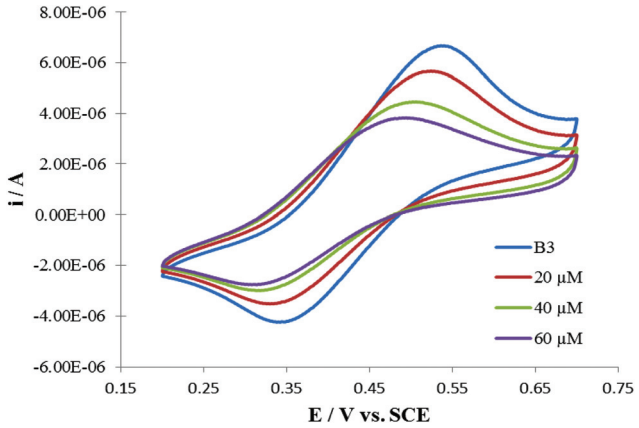

Fig. 8 Cyclic voltammograms of 1 mM B3 recorded at a 0.05 V s^{-1} potential sweep rate on a glassy carbon electrode at 298 K in the absence and presence of 1 mL of increasing concentrations of CT-DNA (10 μM, 20 μM and 60 μM) in a 20% aqueous DMSO buffer at pH 6.0; supporting electrolyte 0.1 M TBAP.

ferrocenium, interacts strongly with DNA. The binding ratio of reduced and oxidized species calculated according to the following equation[32] is given in Table 5.

$$Eb° - Ef° = 0.05916 \log\left(\frac{K_{red}}{K_{oxd}}\right)$$

Eb° and Ef° are the formal potentials of the free and bound forms of the drug respectively. The negative shift indicates that in the case of B16 the oxidized form interacts strongly with DNA whereas in the case of B3 it is the reduced form that interacts more strongly with the DNA. The binding parameters calculated according to the following equation[33] are given in Table 5.

$$\frac{1}{[DNA]} = \frac{K(1-A)}{1-(i/i_0)} - K$$

In the above equation, K is the binding constant, i and i_0 are the peak currents with and without CT-DNA and A is the proportionality constant. The plot of 1/[DNA] *versus* $1/(1 - i/i_0)$ yields binding constants[30] that are given in Table 3. The binding free energy change ($-\Delta G = RT \ln K$) of B16 and B3 in kJ mol^{-1} at 25 °C (Table 5) signifies the spontaneity of drug–DNA interaction.[34]

Studies with pBR322 plasmid DNA

Untreated pBR322 plasmid DNA when electrophoresed for 40 min at room temperature gives two bands corresponding to supercoiled form I and relaxed circular form II. When it is interacted with increasing concentrations of cisplatin ranging from 5 μM to 80 μM, the mobility of both form I and form II bands is found to increase – more so for form II than form I – so that the distance of separation between the bands decreases. The change in mobility of the bands indicates the occurrence of change in DNA conformation believed to be brought about by covalent binding of cisplatin with the DNA. It is known that cisplatin

Table 3 IC_{50} values and resistance factors for cisplatin, B16 and B3

Compounds	A2780 IC_{50} (μM)	A2780^{cisR} IC_{50} (μM)	IC_{50}A2780^{cisR}/IC_{50}A2780 Rf	A2780^{ZD0473R} IC_{50} (μM)	IC_{50}A2780^{cisR}/IC_{50}A2780 Rf
Cisplatin	1.00 ± 0.46	9.95 ± 2.07	9.95	10.22 ± 1.65	10.22
B16	15.27 ± 3.26	16.46 ± 4.13	1.07	17.39 ± 4.93	1.14
B3	17.4 ± 2.02	20.98 ± 5.43	1.21	23.38 ± 6.50	1.34

Table 4 The binding constant, Gibbs free energies and binding ratio of reduced and oxidized species for B16 and B3

Compounds	Binding constant (M^{-1})	$-\Delta G$ (kJ mol^{-1})	K_{red}/K_{oxd}
B16	1.12×10^4	23.10	1.122
B3	1.42×10^2	12.28	0.323

binds with the DNA to form mainly intrastrand bifunctional 1,2-Pt(GG) and 1,2-Pt(AG) adducts that induce the bending of the DNA strand at the binding site.[35] When pBR322 plasmid DNA is interacted with increasing concentrations of B16 and B3 for 40 min at room temperature, no change in intensity and mobility of either the form I or form II band is observed, indicating that the compounds cannot cause any change in DNA conformation, in line with the idea that they do not bind covalently with the DNA (Fig. 9).

BamH1 digestion

Untreated and undigested pBR322 plasmid DNA gave two bands corresponding to forms I and II whereas untreated but BamH1-digested pBR322 plasmid DNA gave a single band corresponding to form III. In the case of pBR322 plasmid DNA interacted with increasing concentrations of cisplatin followed by BamH1 digestion, three bands corresponding to forms I, II and III are seen at all concentrations of the compound. In the case of B16, only a single band corresponding to form III is seen at 5 μM. At higher concentrations of B16 also, a prominent form III can be seen but along with two faint frontal bands. It is believed that the frontal bands are due to DNA fragments produced rather than the form I. In the case of B3, three bands corresponding to forms I, II and III can be seen at all concentrations ranging from 5 μM to 80 μM. The results indicate that cisplatin is much more effective in preventing BamH1 digestion than B16 and B3. This is to be expected since BamH1 cuts the phosphodiester bond between adjacent guanines (specifically it recognizes G/GATTCC)[36] and cisplatin is known to bind with DNA forming an intrastrand bifunctional 1,2-Pt(GG) adduct that causes significant distortion of the DNA strand close to the binding site. Some prevention of BamH1 digestion by B16 and B3 indicates that even non-covalent interactions can induce significant conformational change in the DNA (especially at higher concentrations) so that BamH1 partially fails to recognize the sequence (Fig. 10).

Experimental

Materials and methods

Ferrocene, 4-nitroaniline, sodium nitrite, potassium thiocyanate, acid chlorides such as benzoyl chloride, acetyl chloride, tetrabutylammonium perchlorate (TBAP) and all the other chemicals were purchased from Sigma Aldrich and were used as such. 4-Ferrocenyl-aniline was synthesized by the literature reported method.[37] Solvents such as ethanol, ethyl acetate, acetone, diethyl ether, and petroleum ether were purified before use according to the standard reported protocols. FT-IR and multinuclear (^{1}H and ^{13}C) NMR spectra were obtained using a Thermo Scientific Nicolet-6700 FTIR spectrometer and a BRUKER AVANCE 300 MHz NMR spectrometer.

General synthesis of thiourea

Potassium thiocyanate was dissolved in dried acetone; to this solution acid chloride was added under a N_2 atmosphere. 4-Ferrocenyl aniline was added to the resulting reaction mixture dropwise and stirred for 4 h. The reaction mixture was then poured into ice cooled water and stirred well. The solid product (thiourea) was filtered off and washed with deionized water. The thioureas were dried in air and recrystallized in ethyl acetate.

Synthesis of 1-benzoyl-3-(4-ferrocenylphenyl) thiourea (B16)

Potassium thiocyanate (0.35 g, 3.6 mmol) was dissolved in dried acetone. Benzoyl chloride (0.41 ml, 3.6 mmol) was added to the resulting solution under a N_2 atmosphere. 4-Ferrocenyl aniline (1 g, 3.6 mmol) was added to the resulting reaction mixture and stirred for 4 h. The reaction mixture was then poured into ice cooled water and stirred well. The solid product was filtered off and washed with deionized water. The 1-benzoyl-3-(4-ferrocenylphenyl) thiourea was dried in air and recrystallized in ethyl acetate. **Yield** 73%, **FTIR** (ν **cm^{-1}**): Fe-cp (481 cm^{-1}), NH (3422 cm^{-1}), C═O (1661 cm^{-1}), C═S (1137–1256 cm^{-1}), C═C Ar (1455–1592 cm^{-1}), sp^2 CH (3029.5 cm^{-1}). **^{1}H NMR** (300 MHz, DMSO): δ 12.646 (s, 1H, CSN*H*), 11.57 (s, 1H, CON*H*), 7.99 (s, 4H, C_6H_4), 7.61 (m, 5H, C_6H_5), 4.81 (s, 2H, C_5H_4), 4.36 (s, 2H, C_5H_4), 4.03 (s, 5H, C_5H_5) ppm., **^{13}C NMR** (75 MHz, $CDCl_3$): δ 178.73, 168.73, 137.61, 133.60, 132.61, 129.16, 128.92, 126.39, 124.44, 120.18, 84.62, 69.83, 69.47, 66.77 ppm. **Elemental analysis** Calc. (%) for $C_{24}H_{20}FeN_2OS$: C, 65.46; H, 4.58; N, 6.36; S, 7.28. Found (%): C, 65.32; H, 4.50; N, 6.70; S, 7.21.

Synthesis of 1-acetyl-3-(4-ferrocenylphenyl) thiourea (B3)

B3 was prepared by using the same method as for B16 except using acetyl chloride (0.257 ml, 3.6 mmol) in place of benzoyl chloride. **Yield** 67%, **FTIR** (ν **cm^{-1}**): Fe-cp (481 cm^{-1}), NH (3309 cm^{-1}), C═O (1692 cm^{-1}), C═S (1140–1263 cm^{-1}), C═C Ar (1505–1593 cm^{-1}), sp^2 CH (3037 cm^{-1}), sp^3 CH (2863 cm^{-1}). **^{1}H NMR** (300 MHz, DMSO): δ 11.27 (s, 1H,

Table 5 The intra-molecular and intermolecular hydrogen bond interactions in B16 and B3

Compound	X	H	Y	*d*(X–H) (Å)	*d*(H–Y) (Å)	*d*(X–Y) (Å)	∠(XHY) (°)
Intra-molecular hydrogen bonds							
B16	O1	H1A	N1	1.864(3)	0.861(3)	2.602(5)	142.69(23)
B3	O1	H1A	N1	1.925(4)	0.859(5)	2.648(6)	140.99(29)
Intermolecular hydrogen bonds							
B16	S	H20	C20	2.993	0.929(4)	3.269	98.95
	S	H2A	N2	2.571	0.860(3)	3.376	156.46
B3	S	H2A	N2	2.553	0.860(5)	3.403	169.83
	S	H2A	N2	2.508	0.860(5)	3.358	170.18

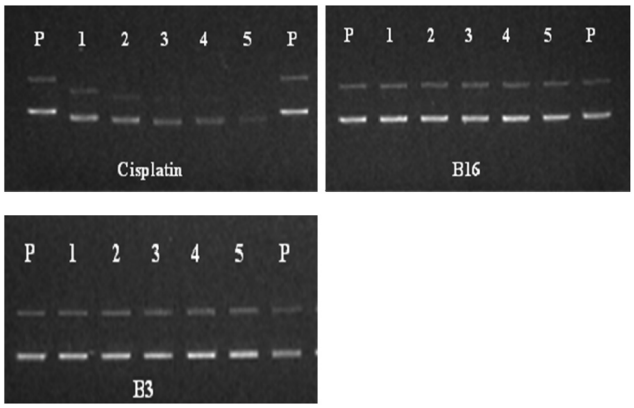

Fig. 9 Electrophoretograms applying to the interaction of pBR322 plasmid DNA with increasing concentrations of cisplatin, B16 and B3. Lane P: untreated pBR322 plasmid DNA to serve as a control; lanes 1 to 5: pBR322 plasmid DNA interacted with increasing concentrations of compounds (cisplatin, B16 and B3) (lane 1: 5 μM; lane 2: 10 μM; lane 3: 20 μM; lane 4: 40 μM; lane 5: 80 μM).

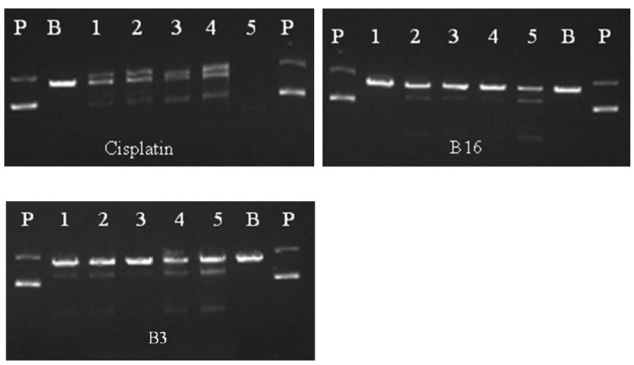

Fig. 10 Electrophoretograms applying to the interaction of pBR322 plasmid DNA with increasing concentrations of cisplatin, B16 and B3 followed by BamH1 digestion. Lane P: untreated and undigested pBR322 plasmid DNA; lane B: untreated but BamH1-digested pBR322 plasmid DNA; lanes 1 to 5: pBR322 plasmid DNA interacted with increasing concentrations of compounds (cisplatin, B16 and B3) (lane 1: 5 μM; lane 2: 10 μM; lane 3: 20 μM; lane 4: 40 μM; lane 5: 80 μM) followed by BamH1 digestion.

CSN*H*), 10.39 (s, 1H, CON*H*), 7.92 (d, J = 7.5 Hz, 2H, C_6H_4), 7.44 (d, J = 7.5 Hz, 2H, C_6H_4), 4.82 (t, J = 1.8 Hz, 2H, C_5H_4), 4.36 (t, J = 1.8 Hz, 2H, C_5H_4), 4.02 (s, 5H, C_5H_5), 2.19 (s, 3H, CH_3) ppm. **^{13}C NMR** (75 MHz, $CDCL_3$): δ 176.59, 171.27, 138.43, 131.92, 127.43, 126.69, 84.33, 70.07, 69.33, 66.73, 25.36 ppm. **Elemental analysis** Calc. (%) for $C_{19}H_{18}FeN_2OS$: C, 60.33; H, 4.80; N, 7.41; S, 8.48. Found (%): C, 60.71; H, 4.91; N, 7.13; S, 8.29.

X-ray structure analysis

X-ray measurements were made on a Bruker kappa APEXII CCD diffractometer equipped with a graphite-monochromated Mo-Kα (λ = 0.71073 Å) radiation source. Data collection used ω scans, and a multi-scan absorption correction was applied. The structure was solved by using the SHELXS97 (Sheldrick, 273 2008) program. The structure was refined by full matrix least-squares techniques using SHELXL-97. The fractional coordinates of B16 and B3 are presented in Table 3.

Cytotoxicity assays

The cytotoxicities of B16 and B3 were screened against human ovarian cell lines: A2780 (parent), A2780^{cisR} (cisplatin-resistant type), A2780^{ZD0473R} (ZD0473-resistant type) using the 3-(4,5-dimethylthiazol-2-yl)-2,5-diphenyltetrazolium bromide (MTT) reduction assay. Cisplatin was used as a control. Briefly between 4000 to 5000 cells were seeded into the wells of the flat-bottomed 96-well culture plate in a 10% FCS/RPMI 1640 culture medium. The plates were incubated for 24 h in a humidified atmosphere (37 °C, 5% carbon dioxide in air, pH 7.4) to allow the cells to attach. Drugs were added at four different concentrations to triplicate wells that were left in the incubator (37 °C, 5% carbon dioxide in air, pH 7.4) for 72 h. After the period, the growth inhibition of cells was determined. 50 μL per well of 1 mg mL^{-1} freshly prepared MTT solution was added to each plate. After 4 h, the formazan crystals formed in each well were dissolved in 150 μL of DMSO and the absorbance of the resulting solution was read using a Bio-Rad Modal 3550 Microplate Reader set at 550 nm.[38]

DNA binding studies

Interaction with CT-DNA

Cyclic voltammetric (CV) measurements were performed in a single compartment cell with a three electrode configuration using an Eco Chemie Auto lab PGSTAT 12 potentiostat/galvanostat (Utrecht, The Netherlands) equipped with the electrochemical software package GPES 4.9. The three electrode system

consisted of Ag/AgCl as the reference electrode, a platinum wire of thickness 0.5 mm with an exposed end of 10 mm as the counter electrode and a bare glassy carbon electrode (surface area of 0.071 cm^2) as the working electrode. The voltammogram of a known volume of the test solution was recorded in the absence of calf thymus DNA (CT-DNA) after flushing out oxygen by purging with argon gas for 10 min just prior to each experiment. The procedure was then repeated for systems with a constant concentration of the drugs (1 mM) and varying concentrations of CT-DNA (20 μM to 60 μM). The working electrode was cleaned after every electrochemical assay. The sodium salt of calf thymus DNA purchased from Acros was used as received. 1 mM stock solutions of B16 and B3 were prepared in 20% aqueous ethanol (20% H_2O : 80% ethanol) and all sample solutions were buffered at pH 6 using a phosphate buffer (0.1 M NaH_2PO_4 + 0.1 M NaOH). Methanol recrystallized tetrabutylammonium perchlorate (TBAP) was used as the supporting electrolyte. The stock solution of CT-DNA (200 μM) was prepared by using doubly distilled water and stored at 4 °C. The concentration of CT-DNA was determined by UV absorbance at 260 nm (molar coefficient ϵ of CT-DNA was taken as 6600 M^{-1} cm^{-1}).[39]

Interaction with pBR322 plasmid DNA

The interaction between pBR322 DNA and B16, B3 and cisplatin was investigated using agarose gel electrophoresis to obtain insight into DNA conformational change. To a fixed concentration (1 μL) of pBR322 plasmid DNA was added increasing concentrations of B16, B3 and cisplatin (5 μM to 80 μM). The total volume was made up to 20 μL by adding mQ water. The resulting solution was incubated on a shaking bath at 37 °C for 4 h. 16 μL aliquots of a drug–DNA mixture were loaded onto the 2% gel and electrophoresis was run under a TAE buffer containing ethidium bromide (1 mg mL^{-1}) for 40 min at 150 V cm^{-1}. The bands of pBR322 plasmid DNA on gel were visualised under short wave UV light using the Bio-Rad Trans illuminator IEC 1010 and photographed.

BamH1 digestion

An identical set of the drug–DNA mixture (as described for interaction with pBR322 plasmid DNA) was incubated for 4 h on a shaking water bath at 37 °C and then subjected to BamH1 digestion. To each 18 μL of the incubated drug–DNA mixture, 2 μL of 10× digestion buffer SB was added followed by 0.1 μL BamH1 (1 unit). The resulting mixtures were kept on a shaking water bath at 37 °C for 1 h after which reactions were stopped by rapid cooling. The gel was photographed by the prescribed method (as used for interaction with pBR322 plasmid DNA).[40]

Conclusions

Two newly synthesized ferrocene incorporated *N*,*N*′-disubstituted thioureas coded as B16 and B3 show significant activity in a number of human ovarian tumour models. The more active compound (B16) undergoes partial intercalation with double helical DNA whereas the less active (B3) undergoes only electrostatic interaction.

Acknowledgements

Bhajan Lal is grateful to the Higher Education Commission Pakistan for the award of an indigenous PhD scholarship combined with an IRSIP scholarship. This research is partly funded by Biomedical Science Research Initiative Grant and Biomedical Science Cancer Research Donation Fund, School of Medical Sciences, The University of Sydney.

References

1 B. Rosenberg, *Platinum Metals Rev.*, 1971, **15**, 42.
2 K. R. Barners and S. J. Lippard, *Met. Ions Biol. Sys.*, 2004, **42**, 143.
3 Z. Guo and P. J. Sadler, *Adv. Inorg. Chem.*, 2000, **49**, 183.
4 D. Wang and S. J. Lippard, *Drug Discovery*, 2005, **4**, 307.
5 E. R. Jamieson and S. J. Lippard, *Chem. Rev.*, 1999, **99**, 2467.
6 M. J. Bloemin and J. Reedijk, *Metal Ions Biol. Sys.*, 1999, **32**, 641.
7 N. P. Farrell, *Semin. Oncol.*, 2004, **31**(Suppl 14), 1.
8 R. A. Alderden, M. D. Hall and T. W. Hambley, *J. Chem. Educ.*, 2006, **83**, 728.
9 T. W. Hambley, *J. Chem. Soc., Dalton Trans.*, 2001, 2711.
10 D. R. Van Staveren and N. Metzler-Nolte, *Chem. Rev.*, 2004, **104**, 5931.
11 M. F. R. Fouda, M. M. Abd-Elzaher, R. A. Abdelsamaia and A. A. Labib, *Appl. Organomet. Chem.*, 2007, **21**, 613.
12 B. Lal, A. Badshah, A. A. Altaf, N. Khan and S. Ullah, *Appl. Organomet. Chem.*, 2011, **25**, 843.
13 C. Sacht and M. S. Datt, *Polyhedron*, 2000, **19**, 1347.
14 S. Neidle, *Prog. Med. Chem.*, 1979, **16**, 151.
15 P. Pigeon, S. Top, O. Zekri, E. A. Hillard, A. Vessieres, M. A. Plamont, O. Buriez, E. Labbe, M. Huche, S. Boutamine, C. Amatore and G. Jaouen, *J. Organomet. Chem.*, 2009, **694**, 895.
16 M. F. R. Fouda, M. M. Abd-Elzaher, R. A. Abdelsamaia and A. A. Labib, *Appl. Organomet. Chem.*, 2007, **21**, 613; and references cited therein.
17 D. Osella, H. Mahboobi, D. Colangelo, G. Caviogiolio, A. Vessie'res and G. Jouen, *Inorg. Chim. Acta*, 2000, **306**, 42.
18 H. Tamura and M. Miwa, *Chem. Lett.*, 1997, **11**, 1177.
19 D. Osella, M. Ferrali, P. Zanello, F. Laschi, M. Fontani, C. Nervi and G. Cavigiolio, *Inorg. Chim. Acta*, 2000, **306**, 42.
20 S. Saeed, N. Rashid, P. G. Jones, M. Ali and R. Hussain, *Eur. J. Med. Chem.*, 2010, **45**, 1323.
21 P. C. Lv, H. Q. Li, J. Sun, Y. Zhu and H. L. Zhu, *Bioorg. Med. Chem.*, 2010, **18**, 4606.
22 H. Q. Li, T. Yan, Y. Yang, L. Shi, C. F. Zhou and H. L. Zhu, *Bioorg. Med. Chem.*, 2010, **18**, 305.
23 A. A. Altaf, A. Badshah, N. Khan and M. N. Tahir, *Acta Crystallogr*, 2010, **E66**, m831.
24 M. K. Rauf, A. Badshah, M. Gielen, M. Ebihara, D. Vos and S. Ahmed, *J. Inorg. Biochem.*, 2009, **103**, 1135.
25 M. K. Rauf, A. Badshah and M. Bolte, *Acta Crystallogr.*, 2006, **62**, o4296.
26 M. K. Rauf, A. Badshah and U. Florke, *Acta Crystallogr.*, 2006, **62**, o2452.
27 F. Javed, A. A. Altaf, A. Badshah, M. N. Tahir, M. Siddiq, Z. U. Rehman, A. Shah, S. Ullah and B. Lal, *J. Coord. Chem.*, 2012, **65**, 969.
28 H. Tayyem, F. Huq, J. Q. Yu, P. Beale and K. Fisher, *Chem. Med. Chem.*, 2008, **3**, 145.
29 G. Tabbi, C. Cassino, G. Cavigiolio, D. Colangelo, A. Ghiglia, I. Viano and D. Osella, *J. Med. Chem.*, 2002, **45**, 5786.
30 A. Shah, M. Zaheer, R. Qureshi, Z. Akhter and M. F. Nazar, *Spectrochim. Acta, Part A*, 2010, **75**, 1082.
31 A. Shah, R. Qureshi, N. K. Janjua, S. Haque and S. Ahmad, *Anal. Sci.*, 2008, **24**, 1437.
32 S. Mahadevan and M. Palaniandavar, *Inorg. Chem.*, 1998, **37**, 693.
33 M. S. Ibrahim, I. S. Shehatta and A. A. Al-Nayeli, *J. Pharm. Biomed. Anal.*, 2002, **28**, 217.

34 J. B. Chaires, S. Satyanarayana, D. Suh, I. Fokt, T. Przewloka and W. Priebe, *Biochemistry*, 1996, **35**, 2047.
35 F. Huq, J. Q. Yu, H. Daghriri and P. Beale, *J. Inorg. Biochem.*, 2004, **98**, 1261.
36 L. A. Smith and Chirikjian, *J. Biol. Chem.*, 1979, **254**, 1003.
37 A. A. Altaf, N. Khan, A. Badshah, B. Lal, S. Ullah, S. Anwar and M. Subhan, *J. Pak. Chem. Soc.*, 2011, **33**, 691.
38 M. U. Nessa, P. Beale, C. Chan, J. Q. Yu and F. Huq, *Anticancer Res.*, 2012, **32**, 53.
39 M. E. Reichmann, S. A. Rice, C. A. Thomas and P. Doty, *J. Am. Soc.*, 1954, **76**, 3047.
40 N. Deqnah, J. Q. Yu, P. Beale, K. Fisher and F. Huq, *Anticancer Res.*, 2012, **32**, 135.